

Article

Phosphorus Mobilizing Enzymes of *Alnus*-Associated Ectomycorrhizal Fungi in an Alaskan Boreal Floodplain

Roger W. Ruess ^{1,*}, Michaela M. Swanson ¹, Knut Kielland ¹, Jack W. McFarland ², Karl D. Olson ¹ and D. Lee Taylor ³

¹ Institute of Arctic Biology, University of Alaska, Fairbanks, AK 99775, USA

² U.S. Geological Survey, Menlo Park, CA 94025, USA

³ Department of Biology, University of New Mexico, Albuquerque, NM 87131, USA

* Correspondence: rwruess@alaska.edu

Received: 1 June 2019; Accepted: 28 June 2019; Published: 2 July 2019



Abstract: Because of its high phosphorus (P) demands, it is likely that the abundance, distribution, and N-fixing capacity of *Alnus* in boreal forests are tightly coupled with P availability and the mobilization and uptake of soil P via ectomycorrhizal fungi (EMF). We examined whether *Alnus* shifts EMF communities in coordination with increasingly more complex organic P forms across a 200-year-old successional sequence along the Tanana River in interior Alaska. Root-tip activities of acid phosphatase, phosphodiesterase, and phytase of *A. tenuifolia*-associated EMF were positively intercorrelated but did not change in a predictable manner across the shrub, to hardwood to coniferous forest successional sequence. Approximately half of all *Alnus* roots were colonized by *Alnicola* and *Tomentella* taxa, and ordination analysis indicated that the EMF community on *Alnus* is a relatively distinct, host-specific group. Despite differences in the activities of the two *Alnus* dominants to mobilize acid phosphatase and phosphodiesterase, the root-tip activities of P-mobilizing enzymes of the *Alnus*-EMF community were not dramatically different from other co-occurring boreal plant hosts. This suggests that if *Alnus* has a greater influence on P cycling than other plant functional types, additional factors influencing P mobilization and uptake at the root and/or whole-plant level must be involved.

Keywords: *Alnus*; phosphorus; ectomycorrhizae; acid phosphatase; phosphodiesterase; phytase; boreal forest; Alaska

1. Introduction

Relative to nitrogen (N), comparatively little is known about terrestrial phosphorus (P) cycling in boreal forests [1,2] despite the tight stoichiometric coupling between N and P in both terrestrial and aquatic ecosystems [3]. During early phases of soil development, P is primarily found in highly reduced inorganic forms of insoluble calcium minerals, such as apatite, which are of limited availability to plants [1]. As soil development progresses, labile inorganic P increases and, for a time, is more available to plants and microbes than in the earliest stages of succession. However, mineral forms become progressively more occluded as Fe and Al oxides [4], and biological activity transforms mineral P into organic forms [5]. Organic P content increases with successional time [6], comprising between 30%–90% of total P in developed soils [7]. Dominant soil organic P compounds include phosphate monoesters (such as phosphorylated sugars and mononucleotides), complex phosphate diesters (predominantly DNA and phospholipids), and more recalcitrant inositol phosphates such as phytic acid [8]. In mid to late soil development, phytates and other large, positively-charged P molecules are tightly bound to soil particles and only available to plants through the release of specialized hydrolyzing enzymes, often with the aid of organic acids.

N-fixing plants play a unique role in P biogeochemical cycling because of the high P demand associated with nitrogenase activity and production of root nodules, which explains the high rates of both N and P cycling in litter of N-fixing plants [9]. How these plants acquire sufficient P to maintain N fixation is somewhat of a puzzle, particularly early in primary succession when N-fixation rates are stimulated by low N and high light availabilities. In old, highly-weathered tropical forests where P availability is often chronically low, it has been suggested that N-fixing plants persist because of their ability to access low-solubility inorganic or recalcitrant organic P forms using extracellular enzymes [10]. In general, extracellular hydrolytic enzymes produced by mycorrhizal associations are a primary mechanism by which plants acquire organic P in soils [11].

Throughout interior Alaska, thin-leaf alder (*Alnus incana* spp *tenuifolia* (Nutt.) Breitung, hereafter, *A. tenuifolia*) forms dense riparian stands where it can contribute $>100 \text{ kg N ha}^{-1} \text{ year}^{-1}$ to early successional floodplain soils through N fixation [9,12,13]. As stands develop, *A. tenuifolia* remains an important understory species in both mid-successional hardwood forests dominated by balsam poplar (*Populus balsamifera* L.), and in late-successional stands dominated by white spruce (*Picea glauca* (Moench) Voss). Field experiments have shown that ecosystem N inputs by *A. tenuifolia* are dramatically increased by P fertilization via increases in both nodule biomass and nitrogenase activity [9,13], suggesting that N fixation rates are strongly P-limited in these ecosystems. The fact that *A. tenuifolia* persists and continues to maintain high nodule biomass and N fixation rates even into late succession [14] suggests this species might change strategies to optimize P access across this successional sequence.

Red alder (*Alnus rubra* Bong.) has been shown to increase inorganic soil P availability via phosphatase production [15]. Furthermore, enzyme activities measured on individual ectomycorrhizal root tips have shown that many species of ectomycorrhizal fungi (EMF) produce phosphohydrolase enzymes when associated with both *Alnus* [16] and other plant hosts [17,18]. In general, EMF community composition is affected by a number of factors, including soil chemistry [19], seasonality [20], and successional stage [21]. *Alnus* associates with a limited number of EMF partners and is often reciprocally selective [22–25], suggesting that the composition of *Alnus*-EMF communities may be tied to the ability of individual fungal species to mobilize various forms of inorganic and organic soil P.

Whereas phosphatase activity is frequently measured on EMF root tips [19,26,27], there is little information as to whether these associations can mobilize P from the more complex forms of organic P in the field, or how this capacity varies among EMF species. Because different enzymes are required for the breakdown of various P forms, hydrolyzing phosphate from compounds such as orthophosphate monoesters, phosphodiester, and phytate may represent different levels of investment. Just as certain non-mycorrhizal plant species may specialize in accessing P from one or more of these forms [28], it is likely that EMF partners have different strategies for acquiring P and may target one source over another. For example, EMF species vary in their capacity to produce phytase [27]; however, compared with the rate of P release from *para*-nitrophenylphosphate, the rate of Pi release from phytate has been shown to be notably less [29].

The objective of this study was to understand the potential for *A. tenuifolia* and its associated EMF partners to mobilize P across spatial (mineral and organic soil horizons) and temporal (chronosequence of successional stages) scales. We hypothesized that: (1) *Alnus*-associated EMF differ in their capacities to mobilize various sources of P, and (2) the variability in EMF enzymatic potential, the community composition of EMF associated with *Alnus*, and the total P-mobilizing potential of the *Alnus*-EMF community are coordinated with spatial and temporal variation in soil resources associated with different stages of boreal forest stand development.

2. Materials and Methods

2.1. Site Description

The Bonanza Creek Long-Term Ecological Research (BNZ LTER) program maintains replicate forest stands representing five stages ($n = 3$ stands/stage) of a 200-year old forest successional sequence along

the Tanana River floodplain 40 km SW of Fairbanks, Alaska, that have been studied intensively for the past 30 years (<http://www.lter.uaf.edu/>). *A. tenuifolia* is the dominant woody species early in succession and persists in the understory in older stands dominated by balsam poplar and, subsequently, white spruce [30]. Mean annual air temperature is -3.3 °C, with average highs of 16.3 °C in July and lows of -45 °C during winter [31]. Soils are cryofluvents and frequently contain buried organic layers resulting from silt deposits during flooding. Across the three sites, soil pH averaged 6.3 and 7.3 in the organic and mineral horizons, respectively. Annual precipitation averages 287 mm, 35% of which falls as snow between October and April. We randomly selected one of the three replicate BNZ LTER stands from the alder (early; 35 years), balsam poplar (mid; 75 years), and white spruce (late; 150 years) stages for sampling. The location of these study sites, referred to with BNZ LTER designators FP1C, BP1 and FP4C, can be viewed at the online BNZ LTER Study Site Catalog (<http://www.lter.uaf.edu/data/sites-catalog>). Our previous studies have demonstrated that variation in alder growth, N fixation, and the identity of *Frankia* partners vary more among individual plants at the 0.1 ha scale within a stand, than they do among replicate stands within a successional stage [9,32,33]. Our sampling design therefore focused on concentrating sampling effort to capture this 0.1 ha-scale variation across the successional gradient, rather than sampling across a larger spatial scale within successional stages.

2.2. Root Tip Selection and Sampling

Plots (30×30 m) were established in stands across a chronosequence including early successional thin-leaf alder, mid-successional balsam poplar, and late successional white spruce stands (hereafter referred to as stages). During August of 2009, one soil core (15×20 cm) was collected approximately 20 cm from the base of 10 randomly chosen alders at each of the four sites. Cores were stored on ice and transported to the lab, where each core was split into mineral and organic horizons. Root systems were washed in cool water and further cleaned of debris under $10\text{--}40\times$ magnification. *Alnus* fine roots were identified by their reddish coloring and the presence of nodules. EMF root tips, between 2–4 mm in length were excised from *Alnus* roots under magnification and stored in 0.5 M CaCl_2 . We collected 50 healthy tips per horizon, and from these, a subsample of seven tips was randomly selected to be assayed for enzymatic activity. Digital pictures of individual root tips were taken through the microscope, and root tip surface areas were determined using root image analysis software Rootfly (Version 1.8.31, 2005–2009, Clemson University). All measurements of enzyme activity are reported per square mm root surface area.

2.3. Enzyme Assays

Within one hour of root tip selection, tips were rinsed of CaCl_2 using 50 mM sodium acetate buffer (pH = 5.5) and run sequentially through a series of assays to assess potential activity of acid phosphatase, phosphodiesterase, and phytase (Appendix A). Individual root tips were placed in sieve strips fabricated from 200 μL tubes which fit snugly into 96-well black-bottomed microplates, and were moved among different microplates for multiple enzyme assays without damage to the root tip [34] (Appendix A). The potential activities of acid phosphatase (AP) and phosphodiesterase (PD) were measured with MU-linked substrates: 6,8-difluoro-4-methylumbelliferyl phosphate (diFMUP, Invitrogen D6567) and Bis (4-methylumbelliferyl) phosphate (bisMUP, BioSynth B-3500), respectively, dissolved in dimethylformamide. Root tips were assayed with two concentrations of each enzyme, diFMUP at 100 μM and 250 μM , and bisMUP at 100 μM and 500 μM . Phytase activity was assayed using the EnzCheck Ultra Phytase Assay Kit (Molecular Probes Inc., Eugene, OR, USA). We used a higher substrate concentration in our phytase assays (2 mM), reflecting the predominance of organic P in many soils which may exceed 200 mg kg^{-1} [35] Fluorescence was read at a wavelength of 360 nm Ex/460 nm Em for both diFMUP and bisMUP and at 540 nm Ex/590 nm Em for phytase on a plate reader (BioTek, Winooski, VT, USA). Incubations were conducted at 20 °C in an environmental chamber and completed within 14 h of soil collection. After incubations, root tips were freeze-dried and stored frozen for molecular analysis.

2.4. Molecular Analyses

To match the enzyme activity with a specific fungal taxon, DNA was extracted from individual root tips using the DNeasy Plant Mini Kit (QIAGEN Inc., Valencia, CA, USA). Prior to extraction, root tips were hydrated in lysis buffer and disrupted using a Kontes pellet pestle attached to a drill. Samples were incubated at 65 °C for 10 min and then for 16 h at 20 °C to improve extraction success. The remainder of the extraction followed the standard protocol for the DNeasy Kit. The EMF species on individual roots tips were identified using Sanger sequencing of the fungal nuclear ribosomal internal transcribed spacer (ITS). This region was amplified using the fungal specific primers ITS1-F and ITS4 [36]. After amplification, PCR products were sent to Functional Biosciences (Madison, WI) for sequencing in both directions (5' and 3') with the same primers. We then assembled sequences, removed ambiguous and poor-quality sequences, and grouped sequences into phylobins that were then assigned a fungal identity [37] (Appendix B). Representative sequences from each phylobin and singletons were used to search the GenBank and UNITE databases. Phylobins were identified to species level at higher than 97% similarity; to the genus level at between 93% and 97%, and to the family level at between 83% and 93% [38]. After initial analysis of the fungal community revealed a wide array of fungi not characteristically detected on *Alnus*, we used restriction length fragment polymorphism (RFLP) to identify the plant host of all samples. This analysis revealed that across all stands, root tips belonged to four plant species: *Alnus tenuifolia* ($n = 151$), *Populus balsamifera* ($n = 30$), *Picea glauca* ($n = 70$), and *Salix spp.* ($n = 19$), and a pool of tips for which host was equivocal ($n = 138$). The latter pool of unidentified host tips is not included in the analyses here.

2.5. Statistical Analyses

All statistical analyses were completed using R statistical software version 3.4.2 [39]. Alpha was set at 0.05, but 0.10 was considered as marginally significant due to low sample size. Outliers were identified as data points above the upper quartile plus three times the inner quartile range, and removed from the final data set prior to analyses. We used mixed-effects models (function *lmer* in the *lmer4* package) to examine the effects of successional stage, soil horizon and their interaction (fixed effects), and plant (random effect) on enzyme activities of alder root tips. Comparisons of models with different fixed effects were made using maximum likelihood, with AIC values compared using *anova* (*lmerTest* package) before refitting models using restricted maximum likelihood. Pairwise comparisons between group members were made using the *lsmeans* function (*lsmeans* package). Assumptions of normality for model residuals were checked using the Shapiro-Wilks normality test (function *shapiro.test*). Acid phosphatase and phosphodiesterase values were square-root transformed, and phytase values were natural log transformed for all models; however, in cases where assumptions of homogeneity were not met, we formulated a variance structure among groups using the *varIdent* function (*nlme* package), and then refit models using *lme* [40]. For model runs that produced a singularity warning, we optimized model performance using the *optimx* function (*optimx* package) and ran models using *lmer*. We report marginal (R^2_m) and conditional (R^2_c) values for models to evaluate variance explained by fixed and fixed+random effects, respectively (*r.squaredGLMM* function). Raw phytase data were strongly bimodal, with a large number of 0 values, and fewer numbers of very high values, which made model interpretations difficult even for those that met assumptions and reached a solution. In this case, we compared groups using the non-parametric Mann-Whitney *U* Test (function *wilcox.test* in the *coin* package). Differences in enzyme activities among dominant alder EMF species, and between ascomycetes versus basidiomycetes across all root tips were assessed using mixed-effects models as described above. Although we unexpectedly ended up with other plant hosts in our final data set, due to unequal sample sizes of those hosts across stages, we could only compare enzyme activities of alder with Salicaceae root tips (*Salix* and balsam poplar root tips pooled) in early succession, and with white spruce in late succession. Non-metric dimensional scaling ordinations of root-tip EMF communities were produced using the *metaNMDS* function in the *vegan* package, using Bray Curtis dissimilarities based on species abundance data grouped by host, successional stage, and horizon.

We then used permutational multivariate analysis of variance to test for differences in root-tip EMF communities among hosts using the *adonis* function (*pairwiseAdonis* package) based on a dissimilarity matrix of species abundance data derived using the function *vegdist*. Throughout the text and Figures, data are presented as means \pm 1 SE.

3. Results

3.1. Alder Root Tip Enzyme Activities

Alder root tip acid phosphatase activity and phosphodiesterase activity showed strong responses to substrate concentration, with rates being approximately double at the higher substrate concentration for both acid phosphatase (6.06 ± 0.35 versus 2.59 ± 0.18 pmoles $\text{min}^{-1} \text{mm}^{-2}$, respectively, $p < 0.01$) and phosphodiesterase (0.75 ± 0.04 versus 0.44 ± 0.02 pmoles $\text{min}^{-1} \text{mm}^{-2}$, respectively, $p < 0.01$) when averaged across all stages. Activities of acid phosphatase (100 and 250 μM) and phosphodiesterase (100 and 500 μM) were positively intercorrelated (all four comparisons, $p < 0.0001$), while phytase activity was positively correlated only with acid phosphatase measured at 250 μM ($p < 0.05$) and phosphodiesterase measured at 100 μM ($p < 0.01$).

Mixed effects model comparisons indicated that modeling enzyme activities as a function of fixed effects (STAGE, HORIZON) and a random intercept effect of PLANT provided the lowest AIC score for all enzymes except for phytase, where the full model (also including the STAGE*HORIZON interaction) was the best fit. Although both STAGE and HORIZON appeared in the best model for all enzymes, most of the explained variance was contributed by the random intercept effect of PLANT in all cases, indicating that variability among plants within stages was more important than either successional stage or horizon in predicting enzyme activities (Figure 1). Acid phosphatase activities of alder root tips measured at both 100 and 250 μM tended to be highest in late successional stages and in organic horizons, but the only statistical differences among stages were found at 250 μM , where mid-successional balsam poplar stands had lower rates than either early or late successional stands (both where the full model (also including the STAGE*HORIZON interaction) was the best fit. $p < 0.05$), which did not differ (Figure 1). In contrast, phosphodiesterase activities were highest in early successional stands when measured at both concentrations. Phytase activity tended to increase across the successional gradient, but differences were not significant. No significant differences were detected for any alder root-tip enzymes harvested from organic versus mineral horizons.

3.2. Comparing Alder Enzyme Activities with Other Host Species

Unequal distribution of root tips from other host species among successional stages restricted comparisons of alder enzyme activities with other hosts to specific sites. In early succession, we compared alder ($n = 52$) and Salicaceae root tips, the latter including both balsam poplar ($n = 15$) and *Salix* sp. ($n = 17$). Alder tended to have lower activities than Salicaceae root tips for all enzymes, although mixed-effects models indicated that differences were only significant for acid phosphatase and phosphodiesterase when measured at high concentrations (Figure 2a). Alder root tips from late successional stands ($n = 44$) had significantly higher activities of acid phosphatase ($p < 0.05$) and tended to have higher phosphodiesterase when measured at low concentrations than did white spruce ($n = 51$), while white spruce tended to have higher activities of phytase (Figure 2b). Mixed effects models failed to resolve differences in phytase activity between alder and Salicaceae, or alder and white spruce. However, Wilcoxon rank sum tests (Mann-Whitney U) indicated that alder had significantly lower phytase activity than Salicaceae ($W = 532.5$, $p < 0.01$) in early succession, and tended to have lower phytase activities than white spruce in late succession ($W = 1350.5$, $p = 0.08$).

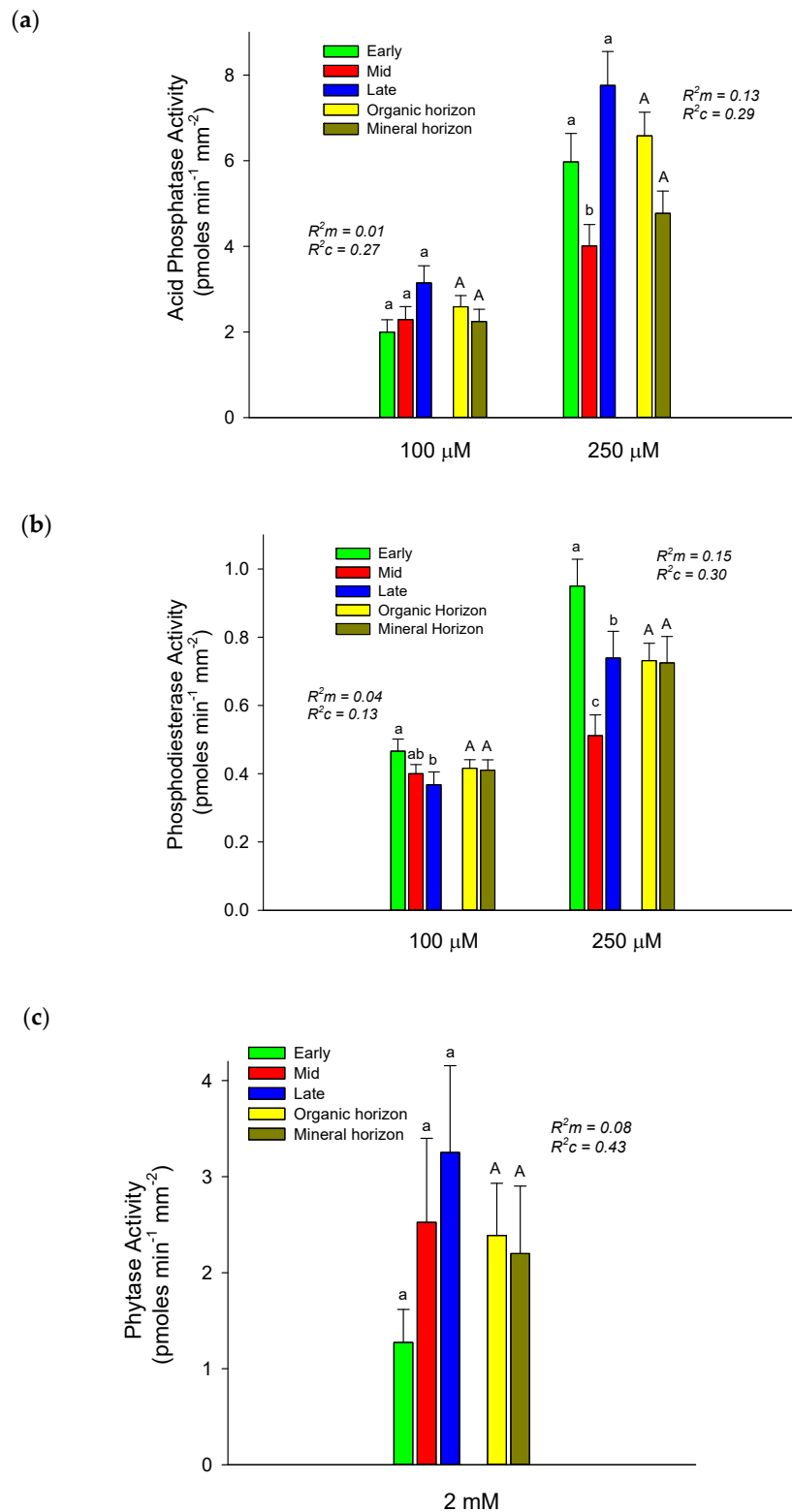
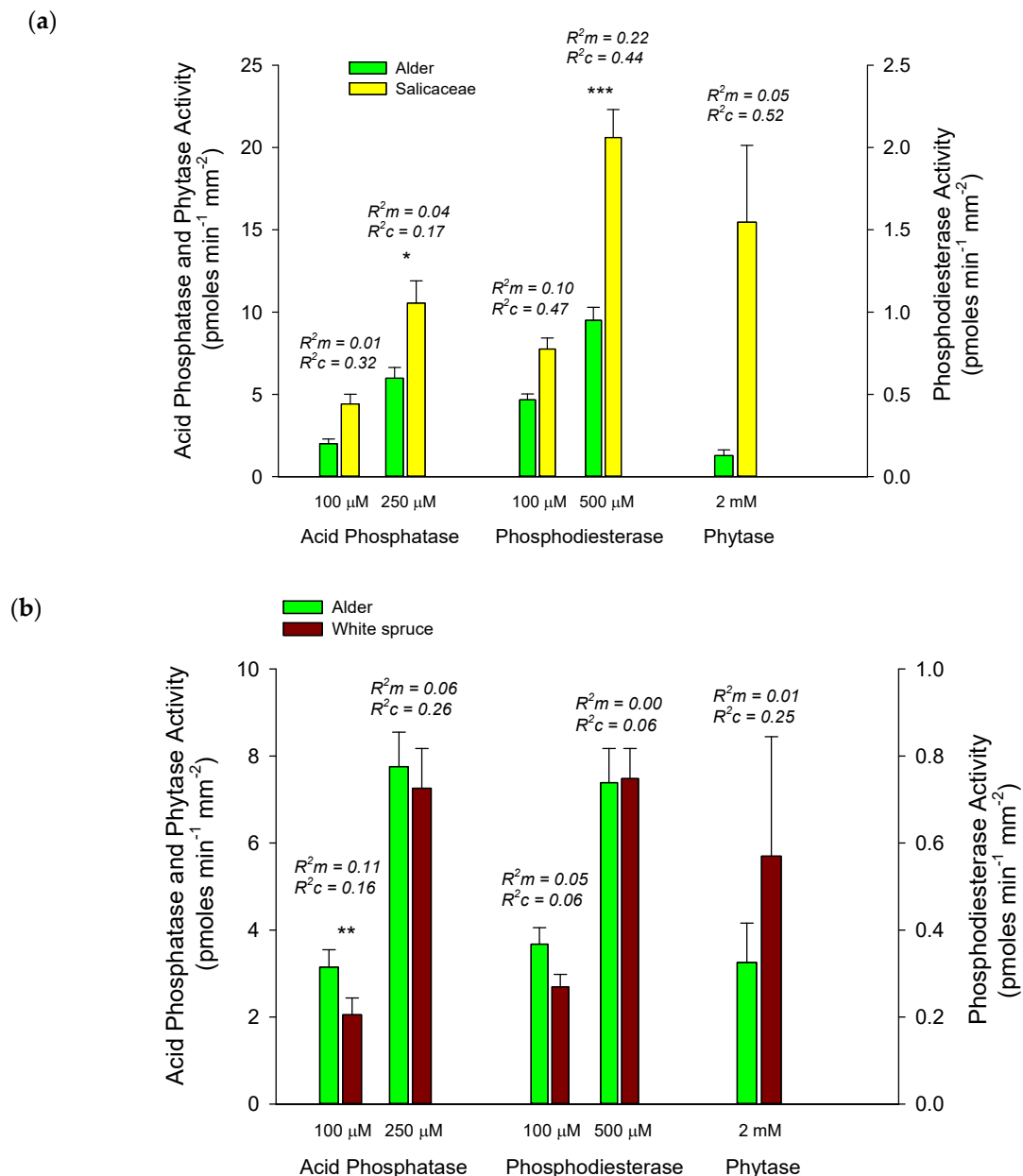


Figure 1. Mean ± S.E. activities of acid phosphatase (a), phosphodiesterase (b), and phytase (c) for thin-leaf alder root tips harvested from organic and mineral horizons from early, mid, and late successional stages. Different lower- and upper-case letters above bars indicate significant differences ($p < 0.05$) between stages and horizons, respectively. Marginal (R^2_m) and conditional (R^2_c) values generated for linear mixed effects models evaluate variance explained by fixed and fixed + random effects, respectively (see Statistics section above).



3.3. Fungal Community Identification

After removal of potential fungal pathogens and non-EMF taxa, we identified 86 unique fungal phylotypes, comprised of 45 basidiomycetes and 41 ascomycetes on 181 roots tips across all plant hosts (Appendix C). The overall fungal community was dominated by basidiomycetes (65%) over ascomycetes (35%). This trend was similar on the 102 *Alnus* roots tips (69% basidiomycetes versus 31% ascomycetes) as well as for *Salix* sp. tips (73% basidiomycetes versus 27% ascomycetes). However, on *Picea* root tips, there tended to be more ascomycetes (61%) than basidiomycetes (39%). No ascomycetes were identified on *Populus* root tips.

Across all hosts, root tips with basidiomycete fungi had significantly higher activities of all enzymes compared with root tips with ascomycete fungi (Figure 3). In general, there was little overlap of dominant fungal species among the EMF communities on different plant hosts (Figure 4). Analyses of fungal communities indicated that EMF fungal community composition varied significantly among hosts ($p < 0.05$), with significant differences between alder and Salicaceae root tips ($p < 0.01$), and between alder and white spruce ($p < 0.10$), but not between Salicaceae and white spruce ($p = 0.45$) (Figure 4). Horizon did not explain any of the variation in fungal community structure, and comparisons among stages, while significant ($p < 0.05$), are difficult to interpret due to unequal representation of host species across stages.

3.4. EMF Specific Activities within and Among Hosts

Low sample sizes and minimal overlap of EMF species among hosts limited our ability to compare enzyme activities of specific EMF species among hosts or among successional stages on a particular host. However, the two dominant alder-associated EMF taxa, *Alnicola luteolofibrillosa* 2 and *Tomentella* sp. 6, which constituted 43% of all alder root tips, showed significant differences in their enzymatic capacity to break down different sources of organic P. Compared to *Alnicola luteolofibrillosa* 2, *Tomentella* sp. 6 showed a greater potential acid phosphatase activity at both the low and high substrate concentrations, whereas *Alnicola luteolofibrillosa* 2 had higher potential phosphodiesterase activity at the higher substrate concentration (Figure 5). Nearly all (96%) of *Alnicola luteolofibrillosa* 2 found on alder root tips occurred in early succession, while *Tomentella* sp. 6, also an alder specialist, was more evenly distributed on alder tips between early (44%) and mid (50%) succession.

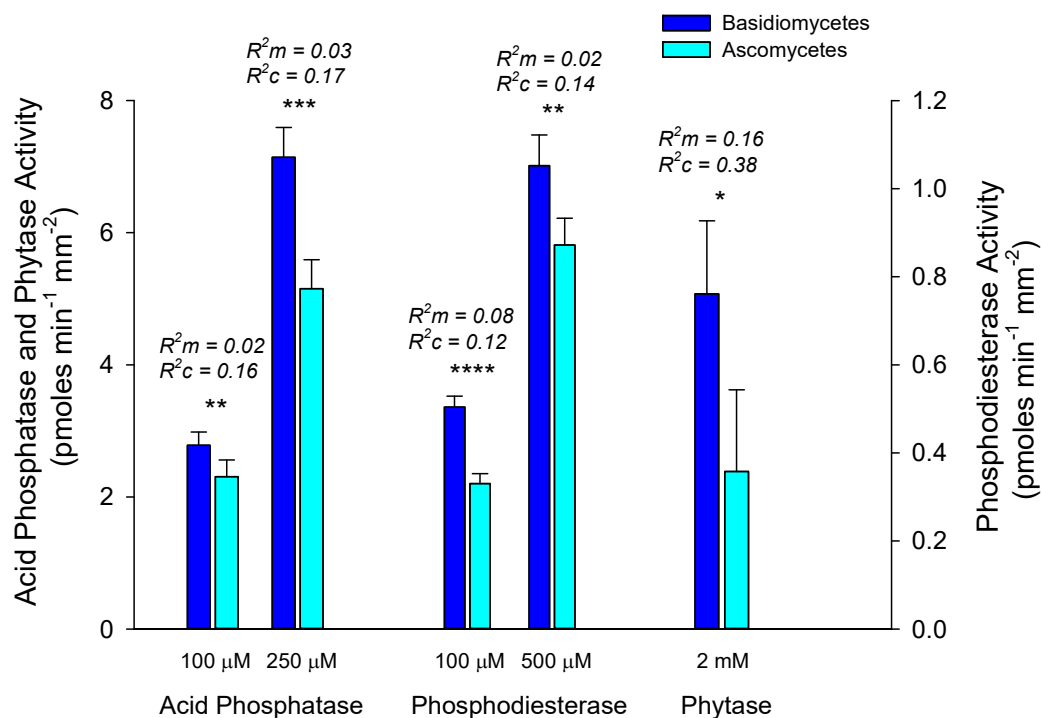


Figure 3. Comparison of mean \pm S.E. activities of acid phosphatase, phosphodiesterase and phytase of alder root tips dominated by Ascomycete versus Basidiomycete ectomycorrhizal fungi (EMF) averaged across all horizons and stages. Significant differences between phylum are indicated above bars at $p < 0.10$ (*), 0.05 (**), 0.01 (***), and 0.001 (****). Marginal (R^2_m) and conditional (R^2_c) values generated for linear mixed effects models evaluate variance explained by fixed and fixed + random effects, respectively (see Statistics section above).

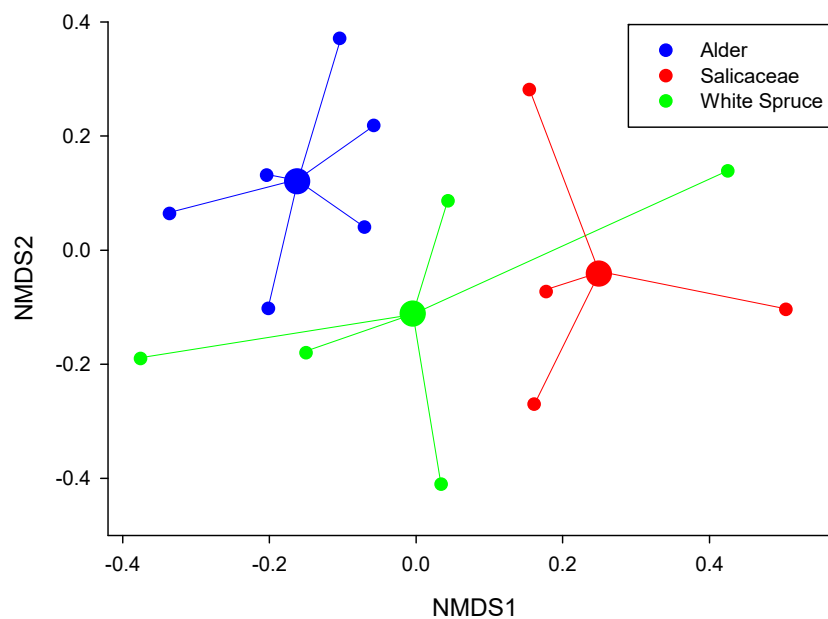


Figure 4. Spider plot of ectomycorrhizal fungi (EMF) community composition derived from non-metric dimensional scaling ordination and PERMANOVA comparisons (*pairwiseAdonis* package) based on a dissimilarity matrix of species abundance data which showed that alder root-tip communities were significantly different from both white spruce ($p < 0.05$) and Salicaceae ($p < 0.10$). Species clusters identify the centroid (spatial mean) of data points representing combinations of successional stage and horizon for each host.

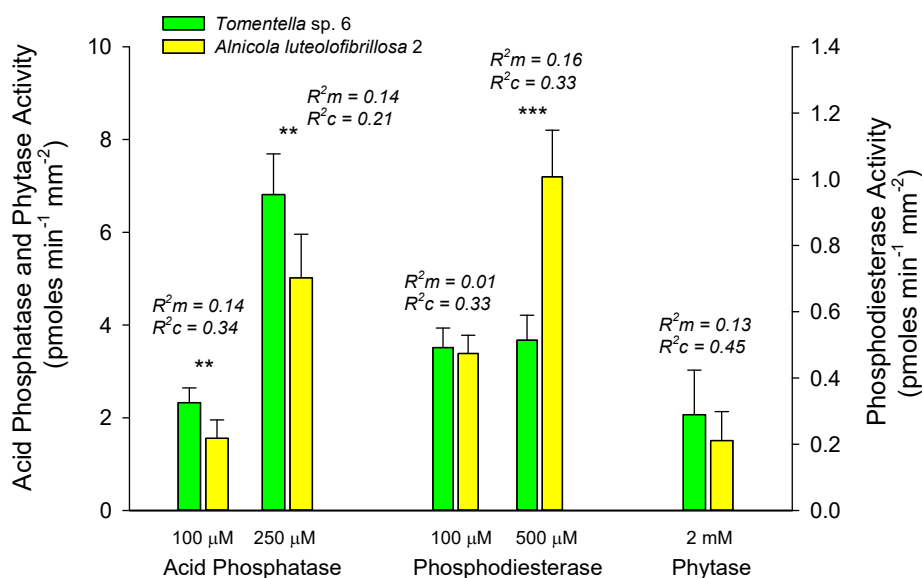


Figure 5. Comparison of mean \pm S.E. activities of acid phosphatase, phosphodiesterase, and phytase of alder root tips dominated by *Tomentella sp. 6* versus *Alnicola luteolofibrillosa 2* averaged across horizons and stages. Significant differences between species are indicated above bars at $p < 0.05$ (**), and 0.01 (***). Marginal (R^2_m) and conditional (R^2_c) values generated for linear mixed effects models evaluate variance explained by fixed and fixed + random effects, respectively (see Statistics section above).

4. Discussion

4.1. Successional Patterns of Root-Tip P Mobilizing Enzymes

We predicted that as soil P is transformed by the biota during primary succession to progressively more recalcitrant organic forms, activities of P-mobilizing enzymes on *Alnus* root tips would shift

towards increases in phosphodiesterase and phytase [41]. We only found partial support for this prediction in that *Alnus* root tips showed a progressive increase in acid phosphatase (100 μ M) and phytase activity across stands. However, phosphodiesterase when measured at low and high substrate concentrations was highest in the early-successional stand, in contrast to the predicted pattern (Figure 1). Recent ^{31}P -NMR data (K.D. Olson) indicate that while the amount of soil organic P increases during succession on an area basis as soil organic C accumulates, concentrations of organic P, and proportions of the dominant forms of inorganic and organic P within organic horizons are actually quite similar across these floodplain successional stages. Thus, the lack of a significant increase in enzymes specifically targeting organic forms of P may not necessarily be unexpected. The fact that rates of P-mobilizing enzymes were positively intercorrelated across all root tips sampled suggests that ectomycorrhizae are using a coordinated suite of enzymes to meet P demands, or perhaps simply that healthier root tips/mycorrhizae have more intact enzymes. Within our early successional stands, organic horizons are poorly developed, with an approximate thickness of 1 cm. Nevertheless, there is a high root density of early successional woody species in surface soils [42], and likely a rapid turnover of organic P from decaying microbes and plant tissues, which may explain why all three enzymes appear to be up-regulated in a coordinated manner to meet plant P demands.

4.2. Differences in Enzyme Activities among Host Species

Motivations behind this study were the strong growth and physiological responses of *A. tenuifolia* to field P-fertilization [9,13], and the suggestion that dominance of N-fixing plants in early successional environments is due in part to their unique capacity to access low-solubility inorganic or recalcitrant organic P forms using extracellular enzymes [10]. Although our original intent was to focus on successional patterns of ectomycorrhizal community composition and P-mobilizing enzyme activities in *Alnus*, root tips of other host species among our samples offer additional insight into whether and how *Alnus* contributes uniquely to P cycling in these ecosystems. In this regard, it is notable that activities of P-mobilizing enzymes were rarely greater and, at times, lower on *Alnus* root tips relative to other hosts (Figure 2), contrary to what would be predicted by the high P demands of *Alnus* [9,43,44], and known capacity of *Alnus* to increase soil P availability [15,45]. Clearly, a more intensive sampling effort targeting other dominant hosts is required to resolve host differences in enzyme activity at the root-tip scale. However, as we point out below, many other factors will influence the stand-level impacts of alder on mobilization and acquisition both inorganic and organic P forms.

4.3. Structure of *Alnus* Ectomycorrhizal Communities

Our results support a growing literature indicating that *Alnus* associates with a relatively low diversity of host-specific ectomycorrhizal fungi of approximately 50–60 species [24]. Moreover, our NMDS/PerMANOVA analyses support the notion that *Alnus* EMF communities are highly distinct relative to other host species [22,46,47]. We identified 38 fungal phylobins on *Alnus*, the majority (55%) in the Phylum Basidiomycota. Of these *Alnus* phylobins, four were found more than four times: *Alnicola luteolofibrillosa* 2 (26 times), *Tomentella* sp. 6 (18 times), *Ascomycete* sp. 3 (six times), and *Phialocephala fortinii* 4 (five times) (Appendix C). Ten rarer types were found between two and three times; three of these 10 were found in more than one stage. The remaining 23 phylobins were detected only once across all sites combined. *Alnicola* and *Tomentella*, the two dominant genera on alder, have been recognized as some of the most common *Alnus*-specific EMF taxa globally [17,22,48]. Individuals from these two genera made up 43% of the total community on *Alnus* across our sites. We also detected species from other EMF genera known to be selective towards *Alnus*, including *Alpova* [22,49,50], *Inocybe* [23], *Tuber* [22], *Lactarius* [49], and *Cortinarius* [16], but did not find other common *Alnus*-specific EMF lineages including/peziza michelii-peziza succosa,/genea-humaria,/pachyphloeus-amylascus, and/tarsetta-geopyxis [22,49].

Although the strong host specificity of EMF on *Alnus* has been repeatedly confirmed, the reasons behind this are less clear. The specificity of host-EMF relationships may result from geographic

isolation; however, some argue that such specialization derives from spatial heterogeneity in soil physical/chemical parameters, and specialization to those conditions [25]. It may be that the unique physiology of N-fixing host species requires EMF partners well suited to facilitating their growth. This could include specialization for P mobilization and uptake, as mentioned above, given the capacity of EMF to aid in P acquisition [51–53]. However, specialization could also be tied to micronutrient acquisition; for instance, Mo, which is required by *Alnus* as a co-factor in the protein complex that reduces atmospheric N₂ [54]. Finally, given that *Alnus* appears to shift *Frankia* partners across successional stages based on their carbon cost relative to N-fixing capacity [9,33], similar market economies may be at play in *Alnus*-EMF communities. Ruess et al. suggested that the up-regulation of nodulation and N-fixation by *Alnus* in P-fertilized plots was enabled by lower carbon partitioning to EMF [9]. The combined costs of having to support both N-fixing bacterial partners and mycorrhizal partners place unique carbon demands on N-fixing plants and suggest that hosts may closely regulate carbon partitioning to EMF mutualists relative to the benefits they afford.

4.4. Patterns of EMF Enzyme Activities

Our analysis of enzyme activities on *Alnus* root tips suggests pronounced physiological differences in the capacity of the two EMF dominants, *A. luteolofibrillosa* 2 and *Tomentella* sp. 6, to mobilize P from compounds across the successional gradient. *A. luteolofibrillosa* 2 had significantly higher phosphodiesterase activities (500 µM) than *Tomentella* sp. 6, while *Tomentella* sp. 6 had significantly higher acid phosphatase activity than *A. luteolofibrillosa* 2 when measured at both high and low substrate concentrations (Figure 5). Differences in the enzyme activities between EMF dominants suggest that these mycorrhizal species differ in their capacity to access P from different substrates and will thus have differing benefits to *Alnus*. There have been few other studies that have tested the functionality of *Alnus*-EMF communities as they relate to P mobilization. However, Walker et al. (2014) [16] found that the potential acid phosphatase activity of the EMF community on *Alnus rubra* was significantly higher than that of Douglas fir (*Pseudotsuga menziesii* (Mirb.) Franco) at two sites in central Oregon. We found a similar tendency for higher acid phosphatase in alder relative to white spruce (Figure 2b). Interestingly, they also found that some of the most dominant fungi in the *Alnus*-EMF community did not demonstrate superior enzymatic activity relative to the community average. Similarly, we found that the higher activities of *A. luteolofibrillosa* 2 versus *Tomentella* sp. 6 for phosphodiesterase and acid phosphatase, respectively, were not significantly greater than the rest of the other EMF species when pooled (data not shown).

Given mixed results across the few studies that have investigated the functionality of *Alnus*-EMF communities, it remains unresolved how *Alnus* meets its P demands and achieves high foliar P concentrations. Our finding that the enzyme activities of *Alnus*-EMF dominants and the *Alnus*-EMF community as a whole are not substantially greater than those found on other plant hosts suggests that if the community of host specific EMF on *Alnus* are related to P mobilization other factors are involved. These could include differences in EMF foraging strategy, extent of hyphal proliferation in the soil, GPP partitioning to first-order root tips and EMF along a branch, EMF growth rate, or P uptake and transport [51], all of which would influence whole-plant P assimilation. Exploration type of the EMF assemblage is likely an important factor influencing P acquisition. There are significant differences in the mantles and exploration types of EMF fungi [55], and EMF taxa vary in the amount of mantle as a proportion of total structure [56]. A given EMF species may have lower enzyme efficiency or infection frequency across root tips, but a more extensive hyphal system that would facilitate access to P from greater distances could result in greater overall P uptake. Additionally, much of the P assimilated by the EMF is retained by the fungus [53,57], despite a high potential for P hydrolysis at the root surface. Differences among EMF species in the proportion of P transferred to the host would not be detected by measuring root tip enzyme activities but may explain some of the specialization we detected in EMF. Future studies are needed to consider the steps between P hydrolysis and assimilation into plant tissue, and the time and scale at which these processes take place, to fully understand EMF-*Alnus* specificity.

The similarity in activity rates of P-mobilizing enzymes measured in the laboratory for *Alnus* growing across very different stand types, and in *Alnus* relative to other dominant woody plant species may not necessarily translate to *in situ* equivalences in the effects that these host species have on P biogeochemical cycling at the stand level. In the field, rates of whole plant P hydrolysis and acquisition are impacted by soil temperature and moisture, root density, plant growth and biomass partitioning, and whole-plant P demands. Average growing season soil temperatures decline from early to mid to late-successional sites, and soil moisture across stand types can be highly variable [9]. In early successional stands where *Alnus* dominates, *in situ* rates of root-tip P-mobilizing enzyme activity rates may be higher than where *Alnus* grows in later successional soils where soil temperature is reduced by mosses, litter, and canopy cover, and soil moisture is often lower due to higher terrace heights. Consistent with greater growth and N-fixation, whole plant P demand, as indexed by higher leaf P concentrations and greater N-fixation responses to P fertilization, is higher in these early-successional, dense stands dominated by *Alnus* [9]. Finally, in both mid- and late-succession, where *A. tenuifolia* grows in the sub-canopy of balsam poplar and white spruce, respectively, light levels are lower, and *Alnus* growth rates and N-fixation rates are reduced relative to early successional stands [9].

4.5. Phytase Activity

Although several studies have assessed the potential of EMF to mobilize P from organic sources [18,51,53], most have focused on acid phosphatase activity [16,19,56,58,59] and to a lesser extent phosphodiesterase activity [6]. Phytase activity has rarely been measured on EMF root tips [27] and never before to our knowledge on *Alnus*, despite the reputedly large proportion of phytate in total soil P pools [8,60]. Reasons behind this may relate to the importance of simple phosphomonoesters as a component of soil organic P. However, this phenomenon may also be methodological; assessing phytase activity on root tips and in soils is difficult. The method we used for measuring phytase activity on root tips has potential to further our understanding of the role of EMF in breaking down complex recalcitrant P molecules, which often make up large proportions of the organic P pool [8,60,61], and may become increasingly important where P is limiting. We were unable to resolve clear differences in phytase activity across succession, between horizons, or hosts; however, we note the high variability of this enzyme activity at all levels, which may suggest large differences among individual EMF species in the capacity to produce phytase.

5. Conclusions

Understanding how host-EMF mutualisms respond to and influence organic soil P fractions is clearly important to broader questions of P biogeochemical cycling in boreal forests. These questions are now approachable given refined methods for the analyses of soil P fractions, enzyme activities, EMF identities, and functional genes. Notwithstanding our low sample size, it is interesting we did not find superior capacity for P mobilization in alder relative to other hosts. However, differences in enzyme activities between the two dominant *Alnus* associated fungi in our study suggest that the unique alder EMF community composition may be coupled with P nutrition through C-N-P stoichiometry and exchange costs/benefits. Many other studies document variations in the enzyme activities of individual EMF, but assessing the enzyme potential at the whole-plant or ecosystem level is more difficult. This is uniquely true for alder because it commonly forms very dense, monospecific stands across early successional floodplains and in other disturbed areas where mineral soils are exposed.

Author Contributions: The following contributions were made by the authors: conceptualization, R.W.R., D.L.T., J.W.M., and K.K.; methodology, D.L.T., M.M.S., K.D.O., R.W.R., K.K.; formal analysis, R.W.R., D.L.T., K.D.O., M.M.S.; investigation, Swanson, R.W.R., K.D.O., D.L.T., J.W.M.; writing—original draft preparation, R.W.R. and M.M.S.; writing—review and editing, R.W.R.; project administration, R.W.R.; funding acquisition, R.W.R., D.L.T., K.K.

Funding: This work was funded by the Center for Global Change, University of Alaska Fairbanks (UAF), and by the National Science Foundation grants to R.W. Ruess (NSF DEB-0641033) and to the Bonanza Creek Long Term Ecological Research Program (NSF DEB-0620579 and DEB-1026415). Additional support was provided by the Institute of Arctic Biology and the Biology and Wildlife Department at UAF.

Acknowledgments: We are grateful to several NSF Research Experiences for Undergraduates students, Ivan Lein, Laurel Lynch, Mitchel Slife, Collin Stackhouse, and Josh Tanner, who spent long hours in challenging conditions to help collect and process samples and assisted with enzyme assays. Greg Breed and Calvin Heslop provided valuable statistical advice.

Conflicts of Interest: The authors declare no conflict of interest.

Appendix A. Enzyme Analyses

Individual root tips were incubated in diFMUP for 10 min per concentration and in bisMUP for 30 min per concentration based on prior testing to optimize enzyme assays. Between incubations in the same substrate, sieve strips were taken out of microplates, blotted on tissue to remove excess substrate, and rinsed for 3 min in wells of sodium acetate buffer. A similar procedure was followed between incubations in different enzyme substrates; however, the rinse incubation time was increased to 10 min. Additionally, sieve strips were gently rinsed under flowing sodium acetate buffer. At the end of the incubation period for each enzyme, 90 μ L of the solution in each well was transferred into new a well containing 10 μ L 0.5 M NaOH to stop the reaction and fluorescence was read immediately.

For phytase, root tips were placed into a reaction mixture containing 50 mM sodium acetate buffer (pH = 5.5), maltose phosphorylase, maltose, glucose oxidase, horseradish peroxidase, Amplex UltraRed dissolved in dimethylsulfoxide, and 2.0 mM phytic acid. Inorganic phosphorus (Pi) released from the hydrolysis of phytic acid during the assay reacts with enzymes in the reaction mixture to form H₂O₂ which reacts with Amplex UltraRed to create a florescent product that is proportional to the amount of Pi released. Wells containing reaction mixture without phytic acid were also included to adjust for autofluorescence of the reaction mixture. Root tips, in sieve strips, were placed in 100 μ L of the reaction mixture for one hour. At the end of the incubation, sieve strips were removed and 65 μ L solution was transferred from each well into a new read plate. Three reference standards were included in each plate. Standards contained the reaction mixture, with 0, 25, 50, 100, 200, 400, 800, and 1600 μ M potassium phosphate replacing the phytic acid in the mixture.

Wells containing substrate without root tips were included in microplates to control for autofluorescence of the substrate. Three reference standards were included in each plate using 0, 0.5, 1, 1.5, 2.5, 3.5, 4.5, and 5.5 mM concentrations of 6,8-difluoro-7-hydroxy-4-methylcoumarin (MU). Standards were used to generate calibration curves that related fluorescence values to the quantity of MU released by the enzyme.

Appendix B. Molecular Characterization of Root Tips

Stock genomic DNA from extracted samples was diluted tenfold. Diluted template (5 μ L) was added to a PCR reaction mixture of 10 \times PCR Buffer (Sigma-Aldrich), 10 mM dNTPs, 25 mM MgCl₂, a 50 mM concentration of each primer and 2.5 KU of Taq polymerase (Sigma-Aldrich, St. Louis, MO, USA). The PCR cycling conditions for those reactions included an initial melt at 94 $^{\circ}$ C for 3 min, followed by 30 cycles of 94 $^{\circ}$ C for 45 s, 55 $^{\circ}$ C for 45 s, and 72 $^{\circ}$ C for 35 s. The program terminated after a final extension at 72 $^{\circ}$ C for 10 min.

Reads were first trimmed and aligned using CodonCode Aligner 3.7 (Dedham, MA, USA) and then assessed for base quality. Low quality bases, with a phred score below 20, were trimmed from ends, low quality bases within sequences were changed to Ns to remove ambiguous sequences, and sequences were oriented. We grouped sequences into phylogenetic clusters at approximately the species level using a script that carries out the following steps [37]. First, sequences are clustered into broad groups using the genome assembly program TGICL [62], which is based on Cap3 [63], with default settings except a percent identity threshold of 90%. All sequences falling into a Cap3 'contig' are then subject to BLAST searches [64] against the database in GenBank. All unique BLAST

matches are added to the file of input sequences for that cluster. Next, the query sequences plus BLAST matches within a cluster are aligned using default parameters in MUSCLE [65]. Then, the best maximum-likelihood phylogenetic tree is sought using the rapid bootstrap protocol in RAxML [66]. Lastly, the script explores the best tree and defines 'phylobins' based on a combination of branch length (defaults: minimum 0.001, maximum = 0.03) and bootstrap support (default: minimum = 70%, maximum = 95%).

As standard references, DNA from all abundant woody plant species found in our plot was extracted from fresh tissue using the DNeasy Plant Mini Kit (Qiagen Inc., Germantown, MD, USA). Prior to extraction, plant tissue was ground by hand using liquid nitrogen. Samples were extracted as described above. The trnL region of the plant chloroplast was amplified using the trnC–trnD primer pair [47,67] using DNA from both the plant tissue controls and from all root tip DNA used in enzyme analysis. The PCR cycling conditions for those reactions included an initial melt at 94 °C for 3 min, followed by 30 cycles of 94 °C for 45 s, 55 °C for 45 s, and 72 °C for 35 s. The program terminated after a final extension at 72 °C for 10 min. PCR products were digested with the TaqI restriction enzyme at 65 °C for 2 h and then run out on 3% agarose gels. Sample fragments were matched to banding patterns of plant standards for host identification.

Appendix C

Table A1. Ectomycorrhizal fungi associated with Alder, Willow, Balsam poplar, White spruce, and unknown host (UNKN) sampled across early, mid and late successional stands along the Tanana River floodplain, Alaska. Tips with unknown hosts were not included in the analyses presented in this manuscript, but are included in this table as a record of what EMF species were recorded at these sites.

Phylobin	Assigned Study Name	Best Match	Phylum	GenBank	UNITE ID	Match	Alignment Length (bp)	Score	Alder	Willow	Balsam Poplar	White Spruce	UNKN
292	<i>Alnicola luteolofibrillosa</i> 1	<i>Alnicola luteolofibrillosa</i>	Basid	JN943976		97.9	714	1234	2	0	0	0	0
297	<i>Alnicola luteolofibrillosa</i> 2	<i>Alnicola luteolofibrillosa</i>	Basid		SH190719.06FU	99	599	1072	26	0	1	1	3
274	<i>Alpova alpestris</i>	<i>Alpova alpestris</i>	Basid		SH241746.06FU	97.24	688	1162	1	0	0	0	0
167	<i>Amphinema</i> sp. 1	<i>Amphinema</i> sp.	Basid		SH229867.06FU	99.8	507	931	1	0	0	0	0
68	<i>Articulospora</i> sp.	uncultured <i>Articulospora</i>	Asco		SH234748.06FU	96.55	464	767	1	0	0	0	0
26	<i>Ascomycete</i> sp. 1	<i>Ascomycete</i> sp.	Asco		SH037210.06FU	91.01	367	488	1	0	0	0	0
27	<i>Ascomycete</i> sp. 2	<i>Ascomycete</i> sp.	Asco		SH037210.06FU	90.44	366	473	0	0	0	1	0
28	<i>Ascomycete</i> sp. 3	<i>Ascomycete</i> sp.	Asco		SH037210.06FU	93.44	673	590	6	0	0	6	4
30	<i>Cadophora finlandica</i> 1	<i>Cadophora finlandica</i>	Asco		SH207167.06FU	98.92	465	830	0	0	0	1	0
31	<i>Cadophora finlandica</i> 2	<i>Cadophora finlandica</i>	Asco		SH207167.06FU	98.07	466	809	0	0	0	1	0
364	<i>Cadophora luteo-olivacea</i>	<i>Cadophora luteo-olivacea</i>	Asco		SH204718.06FU	97.24	544	918	0	0	0	0	1
376	<i>Cenococcum geophilum</i>	<i>Cenococcum geophilum</i>	Asco	JN943893		97.61	964	1648	0	0	0	0	1
139	<i>Chalara holubovae</i>	<i>Chalara holubovae</i>	Asco		SH209190.06FU	97.78	451	773	0	0	0	0	1
141	<i>Chalara microchona</i>	<i>Chalara microchona</i>	Asco	DQ093752		98.9	451	778	0	0	0	1	0
64	<i>Cladophialophora</i> sp. 1	uncultured <i>Cladophialophora</i>	Asco		SH025802.06FU	98.22	506	885	1	0	0	0	0
103	<i>Cortinariaceae</i> sp. 1	<i>Alnicola luteolofibrillosa</i>	Basid		SH190719.06FU	89.93	606	767	0	0	0	0	1
104	<i>Cortinariaceae</i> sp. 2	<i>Alnicola luteolofibrillosa</i>	Basid	JN943976		90.26	688	878	1	0	0	0	0
238	<i>Cortinariaceae</i> sp. 3	<i>Cortinariaceae</i> sp.	Basid		SH232566.06FU	99.02	612	1096	0	0	0	1	0
207	<i>Cortinarius casimiri</i> 1	<i>Cortinarius casimiri</i>	Basid		SH232912.06FU	96.08	510	830	0	0	0	1	0
208	<i>Cortinarius casimiri</i> 2	<i>Cortinarius casimiri</i>	Basid		SH232830.06FU	99.41	507	920	0	0	0	1	1
237	<i>Cortinarius cephalixu</i>	<i>Cortinarius cephalixu</i>	Basid	AY174784		99.29	708	1279	1	0	0	0	0
199	<i>Cortinarius</i> sp. 1	<i>Cortinarius subsertipes</i>	Basid	HQ604709		96.75	615	1020	0	0	2	0	3
183	<i>Cyathicula microspora</i>	<i>Cyathicula microspora</i>	Asco		SH014066.06FU	99.36	469	850	0	0	0	0	1
34	<i>Geomyces</i> sp. 1	<i>Geomyces destructans</i>	Asco	EU854569		96.73	888	1476	0	1	0	0	1
129	<i>Gloeotinia temulenta</i>	<i>Gloeotinia temulenta</i>	Asco		SH235673.06FU	99.8	506	928	2	0	0	2	2
349	<i>Gyoerffyella</i> sp. 1	<i>Gyoerffyella</i> sp.	Asco		SH234755.06FU	97.35	452	765	1	0	0	0	2
1	<i>Helotiaceae</i> sp. 1	<i>Leohumicola minima</i>	Asco	AY706329		91.95	559	765	0	0	0	2	0
92	<i>Helotiaceae</i> sp. 2	<i>Helotiaceae</i> sp.	Asco	HQ157915		93.11	537	784	0	0	0	0	1
180	<i>Helotiaceae</i> sp. 3	uncultured <i>Helotiaceae</i>	Asco		SH030055.06FU	97.38	458	774	0	0	0	1	0
377	<i>Helotiaceae</i> sp. 4	<i>Helotiales</i> sp.	Asco		SH444216.06FU	87.31	536	592	2	0	0	0	0
329	<i>Helotiales</i> sp. 1	<i>Leptodontidium</i> sp.	Asco		SH034136.06FU	99.06	531	953	0	0	0	0	1
347	<i>Hyaloscyphaceae</i> sp. 1	<i>Calycina languida</i>	Asco		SH208263.06FU	90.74	475	638	0	0	0	1	0
175	<i>Hygrophorus pustulatus</i>	<i>Hygrophorus pustulatus</i>	Basid	FJ845412		99.8	501	920	0	0	0	1	0
282	<i>Inocybaceae</i> sp. 1	<i>Inocybaceae</i> sp.	Basid		SH240210.06FU	99.31	583	1051	1	0	1	0	0
6	<i>Lachnum</i> sp. 1	uncultured <i>Lachnum</i>	Asco		SH189775.06FU	97.44	468	795	3	0	0	3	1

Table A1. Cont.

Phylobin	Assigned Study Name	Best Match	Phylum	GenBank	UNITE ID	Match	Alignment Length (bp)	Score	Alder	Willow	Balsam Poplar	White Spruce	UNKN
89	<i>Lactarius lilacinus</i>	<i>Lactarius lilacinus</i>	Basid		SH238120.06FU	99.21	630	1136	2	0	0	0	0
284	<i>Leohumicola minima</i>	<i>Leohumicola minima</i>	Asco	AY706329		97.27	549	928	1	0	0	0	0
357	<i>Leptodontidium orchidicola</i> 1	<i>Leptodontidium orchidicola</i>	Asco	AF486133		98.93	652	1168	0	0	0	0	5
359	<i>Leptodontidium orchidicola</i> 2	<i>Leptodontidium orchidicola</i>	Asco	AF486133		97.85	650	1118	0	0	0	0	1
360	<i>Leptodontidium orchidicola</i> 3	<i>Leptodontidium orchidicola</i>	Asco	AF486133		98.29	644	1125	1	0	0	0	0
361	<i>Leptodontidium orchidicola</i> 4	<i>Leptodontidium orchidicola</i>	Asco	AF486133		98.59	638	1127	0	0	0	0	1
363	<i>Leptodontidium orchidicola</i> 5	<i>Leptodontidium orchidicola</i>	Asco	AF486133		98.9	637	1138	0	0	0	0	1
14	<i>Lycoperdon foetidum</i>	<i>Lycoperdon foetidum</i>	Basid		SH244736.06FU	97.42	658	1120	1	0	0	0	0
76	<i>Meliniomyces bicolor</i>	<i>Meliniomyces bicolor</i>	Asco		SH207170.06FU	99.79	475	872	1	0	0	0	0
46	<i>Phialocephala fortinii</i> 1	<i>Phialocephala fortinii</i>	Asco		SH213468.06FU	98.32	476	833	0	0	0	1	0
47	<i>Phialocephala fortinii</i> 2	<i>Phialocephala fortinii</i>	Asco		SH213468.06FU	98.82	592	1055	2	0	0	0	0
49	<i>Phialocephala fortinii</i> 3	<i>Phialocephala fortinii</i>	Asco		SH213468.06FU	98.95	476	850	1	0	0	0	0
339	<i>Phialocephala fortinii</i> 4	<i>Phialocephala fortinii</i>	Asco		SH213468.06FU	97.69	477	824	5	0	0	2	1
366	<i>Phialocephala lagerbergii</i>	<i>Phialocephala lagerbergii</i>	Asco		SH204727.06FU	99.2	500	900	0	0	0	0	1
320	<i>Piloderma</i> sp. 1	<i>Piloderma</i> sp.	Basid	UDB001733		100	621	1147	1	0	0	1	0
128	<i>Plectosphaerellaceae</i> sp.	<i>Verticillium leptobactrum</i>	Asco		SH235676.06FU	94.11	475	715	0	0	0	0	1
61	<i>Russula cessans</i>	<i>Russula cessans</i>	Basid	FJ845437		98.92	646	1151	0	0	0	2	0
59	<i>Russula</i> sp. 1	<i>Russula cessans</i>	Basid	FJ845437		93.32	704	1044	0	0	0	1	0
60	<i>Russula</i> sp. 2	<i>Russula cessans</i>	Basid	FJ845437		94.64	634	976	1	0	0	0	0
380	<i>Russula</i> sp. 3	<i>Russula cessans</i>	Basid	FJ845437		95.04	605	941	0	0	0	1	0
262	<i>Russula versicolor</i>	<i>Russula versicolor</i>	Basid		SH224391.06FU	98.69	610	1081	0	0	0	0	2
343	<i>Sebacina dimitica</i>	<i>Sebacina dimitica</i>	Basid		SH231629.06FU	98.49	530	931	0	0	0	0	1
85	<i>Sebacina epigaea</i>	<i>Sebacina epigaea</i>	Basid	EU819519		95.69	532	907	0	6	0	1	0
119	<i>Sebacina</i> sp. 2	<i>Sebacina</i> sp.	Basid		SH305078.06FU	98.3	529	926	0	3	8	0	1
159	<i>Sebacina</i> sp. 3	<i>Sebacina</i> sp.	Basid		SH231609.06FU	99.25	534	963	1	0	0	0	0
161	<i>Sebacina</i> sp. 4	<i>Sebacina</i> sp.	Basid		SH231664.06FU	98.71	541	957	3	0	0	0	0
344	<i>Sebacina</i> sp. 5	<i>Sebacina</i> sp.	Basid		SH231595.06FU	99.26	541	977	0	0	1	0	3
24	<i>Tetracladium maxilliforme</i>	<i>Tetracladium maxilliforme</i>	Asco	EU883429		97.13	593	1000	2	0	0	0	0
100	<i>Thelephora terrestris</i>	<i>Thelephora terrestris</i>	Basid	HM189958		93.22	708	1031	3	0	0	0	0
20	<i>Thelephoraceae</i> sp. 1	<i>Thelephoraceae</i> sp.	Basid		SH195974.06FU	94.75	590	917	0	0	0	0	1
21	<i>Thelephoraceae</i> sp. 2	<i>Thelephoraceae</i> sp.	Basid		SH195974.06FU	93	586	848	1	0	0	0	0
99	<i>Thelephoraceae</i> sp. 3	<i>Thelephoraceae</i> sp.	Basid		SH219843.06FU	95.52	536	856	1	0	0	0	0
132	<i>Tomentella ferruginea</i> 1	<i>Tomentella ferruginea</i>	Basid	AF272909		98.74	555	985	0	1	0	1	0
134	<i>Tomentella ferruginea</i> 2	<i>Tomentella ferruginea</i>	Basid	AF272909		98.17	546	952	0	0	5	0	2
7	<i>Tomentella</i> sp. 1	<i>Tomentella</i> sp.	Basid		SH213382.06FU	99.65	576	1055	2	0	0	0	0
239	<i>Tomentella</i> sp. 10	<i>Tomentella ellisii</i>	Basid		SH222911.06FU	96.61	590	977	1	0	0	0	0
264	<i>Tomentella</i> sp. 12	uncultured <i>Tomentella</i>	Basid		SH202475.06FU	97.74	576	992	0	0	0	0	1
269	<i>Tomentella</i> sp. 13	<i>Tomentella</i> sp.	Basid	U83482		96.05	683	1110	1	0	0	0	0
379	<i>Tomentella</i> sp. 14	<i>Tomentella</i> sp.	Basid		SH202538.06FU	99.15	587	1055	0	1	0	0	0
8	<i>Tomentella</i> sp. 2	uncultured <i>Tomentella</i>	Basid		SH199023.06FU	98.78	572	1016	0	0	2	3	2
22	<i>Tomentella</i> sp. 6	<i>Tomentella subilacina</i>	Basid	HM189994		95.83	695	1120	18	0	0	1	0

Table A1. Cont.

Phylobin	Assigned Study Name	Best Match	Phylum	GenBank	UNITE ID	Match	Alignment Length (bp)	Score	Alder	Willow	Balsam Poplar	White Spruce	UNKN
98	<i>Tomentella</i> sp. 7	uncultured <i>Tomentella</i>	Basid		SH021829.06FU	94.67	582	896	0	0	0	0	1
223	<i>Tomentella</i> sp. 9	uncultured <i>Tomentella</i>	Basid		SH219870.06FU	98.14	590	1027	0	0	0	0	2
224	<i>Tomentella viridula</i>	<i>Tomentella viridula</i>	Basid	AF272914		99.66	581	1061	0	0	0	0	1
280	<i>Tomentellopsis</i> sp. 1	<i>Tomentellopsis submollis</i>	Basid		SH199523.06FU	96.98	597	1009	1	0	0	0	0
192	<i>Trichophaea</i> sp. 1	<i>Trichophaea cf hybrida</i>	Asco		SH227980.06FU	100	522	965	1	0	0	0	0
10	<i>Tuber</i> sp. 1	uncultured <i>Tuber</i>	Asco		SH204354.06FU	99.66	592	1081	0	3	0	5	0
62	<i>Tuber</i> sp. 2	<i>Tuber rapaeodorum</i>	Asco	EU784430		95.88	582	937	1	0	0	0	0
384	<i>Tuber</i> sp. 3	uncultured <i>Tuber</i>	Asco		SH204354.06FU	99.66	592	1081	0	0	0	0	1
41	<i>Vibrisseaceae</i> sp. 1	<i>Phialocephala fortinii</i>	Asco		SH016932.06FU	84.11	151	147	0	0	0	0	1
150	<i>Wilcoxina rehmsii</i> 2	<i>Wilcoxina rehmsii</i>	Asco		SH023929.06FU	97.58	455	778	0	0	0	1	0

References

1. Marion, G.M.; Van Cleve, K.; Dyrness, C.T.; Black, C.H. The soil chemical environment along a primary successional sequence on the Tanana River floodplain, interior Alaska. *Can. J. For. Res.* **1993**, *23*, 923–927. [[CrossRef](#)]
2. Giesler, R.; Petersson, T.; Hogberg, P. Phosphorus limitation in boreal forests: Effects of aluminum and iron accumulation in the humus layer. *Ecosystems* **2002**, *5*, 300–314. [[CrossRef](#)]
3. Sterner, R.W.; Elser, J.J. *Ecological Stoichiometry: The Biology of Elements from Molecules to the Biosphere*; Princeton University Press: Princeton, NJ, USA, 2002.
4. Walker, T.W.; Syers, J.K. The fate of phosphorus during pedogenesis. *Geoderma* **1976**, *1*, 1–19. [[CrossRef](#)]
5. Crews, T.E.; Kitayama, K.; Fownes, J.H.; Riley, R.H.; Herbert, D.A.; Mueller-Dombois, D.; Vitousek, P.M. Changes in soil phosphorus fractions and ecosystem dynamics across a long chronosequence in Hawaii. *Ecology* **1995**, *76*, 1407–1424. [[CrossRef](#)]
6. Allison, V.J.; Condon, L.M.; Peltzer, D.A.; Richardson, S.J.; Turner, B.L. Changes in enzyme activities and soil microbial community composition along carbon and nutrient gradients at the Franz Josef chronosequence, New Zealand. *Soil Biol. Biochem.* **2007**, *39*, 1770–1781. [[CrossRef](#)]
7. Harrison, A.F. Labile organic phosphorus mineralization in relationship to soil properties. *Soil Biol. Biochem.* **1982**, *14*, 343–351. [[CrossRef](#)]
8. Turner, B.L.; Condon, L.M.; Richardson, S.J.; Peltzer, D.A.; Allison, V.J. Soil organic phosphorus transformations during pedogenesis. *Ecosystems* **2007**, *10*, 1166–1181. [[CrossRef](#)]
9. Ruess, R.W.; Anderson, M.D.; McFarland, J.M.; Kielland, K.; Olson, K.; Taylor, D.E. Ecosystem-level consequences of symbiotic partnerships in a N₂-fixing shrub from interior Alaskan floodplains. *Ecol. Monogr.* **2013**, *83*, 177–194. [[CrossRef](#)]
10. Houlton, B.Z.; Wang, Y.P.; Vitousek, P.M.; Field, C.B. A unifying framework for dinitrogen fixation in the terrestrial biosphere. *Nature* **2008**, *454*, 327–334. [[CrossRef](#)]
11. Smith, S.E.; Read, D.J. *Mycorrhizal Symbiosis*, 3rd ed.; Academic Press: London, UK, 2008.
12. Ruess, R.W.; McFarland, J.M.; Trummer, L.M.; Rohrs-Richey, J.K. Disease-mediated declines in N-fixation inputs by *Alnus tenuifolia* to early-successional floodplains in interior and south-central Alaska. *Ecosystems* **2009**, *12*, 489–501. [[CrossRef](#)]
13. Uliassi, D.D.; Ruess, R.W. Limitations to symbiotic nitrogen fixation in primary succession on the Tanana River floodplain, Alaska. *Ecology* **2002**, *83*, 88–103. [[CrossRef](#)]
14. Anderson, M.D.; Ruess, R.W.; Uliassi, D.D.; Mitchell, J.S. Estimating N₂ fixation in two species of *Alnus* in interior Alaska using acetylene reduction and ¹⁵N₂ uptake. *Ecoscience* **2004**, *11*, 102–112. [[CrossRef](#)]
15. Giardina, C.P.; Huffman, S.; Binkley, D.; Caldwell, B.A. Alders increase soil phosphorus availability in a Douglas-fir plantation. *Can. J. For. Res.* **1995**, *25*, 1652–1657. [[CrossRef](#)]
16. Walker, J.K.M.; Cohen, H.; Higgins, L.M.; Kennedy, P.G. Testing the link between community structure and function for ectomycorrhizal fungi involved in a global tripartite symbiosis. *New Phytol.* **2014**, *202*, 287–296. [[CrossRef](#)] [[PubMed](#)]
17. Pritsch, K.; Munch, J.C.; Buscot, F. Morphological and anatomical characterisation of black alder *Alnus glutinosa* (L.) Gaertn. ectomycorrhizas. *Mycorrhiza* **1997**, *7*, 201–216. [[CrossRef](#)]
18. Plassard, C.; Louche, J.; Ali, M.A.; Duchemin, M.; Legname, E.; Cloutier-Hurteau, B. Diversity in phosphorus mobilisation and uptake in ectomycorrhizal fungi. *Ann. For. Sci.* **2011**, *68*, 33–43. [[CrossRef](#)]
19. Courty, P.E.; Pritsch, K.; Schloter, M.; Hartmann, A.; Garbaye, J. Activity profiling of ectomycorrhiza communities in two forest soils using multiple enzymatic tests. *New Phytol.* **2005**, *167*, 309–319. [[CrossRef](#)]
20. Koide, R.T.; Courty, P.E.; Garbaye, J. Research perspectives on functional diversity in ectomycorrhizal fungi. *New Phytol.* **2007**, *174*, 240–243. [[CrossRef](#)]
21. Tedersoo, L.; Suvi, T.; Jairus, T.; Kõljalg, U. Forest microsite effects on community composition of ectomycorrhizal fungi on seedlings of *Picea abies* and *Betula pendula*. *Environ. Microbiol.* **2008**, *10*, 1189–1201. [[CrossRef](#)]
22. Tedersoo, L.; Suvi, T.; Jairus, T.; Ostonen, I.; Polme, S. Revisiting ectomycorrhizal fungi of the genus *Alnus*: Differential host specificity, diversity and determinants of the fungal community. *New Phytol.* **2009**, *182*, 727–735. [[CrossRef](#)]

23. Kennedy, P.G.; Hill, L.T. A molecular and phylogenetic analysis of the structure and specificity of *Alnus rubra* ectomycorrhizal assemblages. *Fungal Ecol.* **2010**, *3*, 195–204. [[CrossRef](#)]
24. Pölme, S.; Bahram, M.; Yamanaka, T.; Nara, K.; Dai, Y.C.; Grebenc, T.; Kraigher, H.; Toivonen, M.; Wang, P.H.; Matsuda, Y.; et al. Biogeography of ectomycorrhizal fungi associated with alders (*Alnus* spp.) in relation to biotic and abiotic variables at the global scale. *New Phytol.* **2013**, *198*, 1239–1249. [[CrossRef](#)]
25. Roy, M.; Rochet, J.; Manzi, S.; Jargeat, P.; Gryta, H.; Moreau, P.A.; Gardes, M. What determines *Alnus*-associated ectomycorrhizal community diversity and specificity? A comparison of host and habitat effects at a regional scale. *New Phytol.* **2013**, *198*, 1228–1238. [[CrossRef](#)] [[PubMed](#)]
26. Kroehler, C.J.; Linkins, A.E. The root surface phosphatases of *Eriophorum vaginatum*: Effects of temperature, pH, substrate concentration and inorganic phosphorus. *Plant Soil* **1988**, *105*, 3–10. [[CrossRef](#)]
27. Colpaert, J.V.; Van Laere, A.; Van Tichelen, K.K.; Van Assche, J.A. The use of inositol hexaphosphate as a phosphorus source by mycorrhizal and non-mycorrhizal Scots Pine (*Pinus sylvestris*). *Funct. Ecol.* **1997**, *11*, 407–415. [[CrossRef](#)]
28. Turner, B.L. Resource partitioning for soil phosphorus: a hypothesis. *J. Ecol.* **2008**, *96*, 698–702. [[CrossRef](#)]
29. Louche, J.; Ali, M.A.; Cloutier-Hurteau, B.; Sauvage, F.X.; Quiquampoix, H.; Plassard, C. Efficiency of acid phosphatases secreted from the ectomycorrhizal fungus *Hebeloma cylindrosporum* to hydrolyse organic phosphorus in podzols. *FEMS Microbiol. Ecol.* **2010**, *73*, 323–335. [[CrossRef](#)] [[PubMed](#)]
30. Hollingsworth, T.N.; Lloyd, A.H.; Nossov, D.; Ruess, R.W.; Charlton, B.A.; Kielland, K. Twenty-five years of vegetation change along a putative successional chronosequence on the Tanana River, Alaska. *Can. J. For. Res.* **2010**, *40*, 1273–1287. [[CrossRef](#)]
31. Viereck, L.A.; Vancleve, K.; Adams, P.C.; Schlentner, R.E. Climate of the Tanana River floodplain near Fairbanks, Alaska. *Can. J. For. Res.* **1993**, *23*, 899–913. [[CrossRef](#)]
32. Anderson, M.D.; Ruess, R.W.; Taylor, D.L.; Myrold, D.D. Host species and habitat affect nodulation by specific *Frankia* genotypes in two species of *Alnus* in interior Alaska. *Oecologia* **2009**, *160*, 619–630. [[CrossRef](#)]
33. Anderson, M.D.; Taylor, D.E.; Ruess, R.W. Phylogeny and assemblage composition of *Frankia* in *Alnus tenuifolia* nodules across a primary successional sere in interior Alaska. *Mol. Ecol.* **2013**, *22*, 3864–3877. [[CrossRef](#)] [[PubMed](#)]
34. Pritsch, K.; Raidl, S.; Marksteiner, E.; Blaschke, H.; Agerer, R.; Schloter, M.; Hartmann, A. A rapid and highly sensitive method for measuring enzyme activities in single mycorrhizal tips using 4-methylumbelliferone-labelled fluorogenic substrates in a microplate system. *J. Microbiol. Methods* **2004**, *58*, 233–241. [[CrossRef](#)] [[PubMed](#)]
35. Giles, C.D.; Cade-Menun, B.J.; Hill, J.E. The inositol phosphates in soils and manures: Abundance, cycling, and measurement. *Can. J. Soil Sci.* **2011**, *91*, 397–416. [[CrossRef](#)]
36. Gardes, M.; Bruns, T.D. ITS primers with enhanced specificity for basidiomycetes - application to the identification of mycorrhizae and rusts. *Mol. Ecol.* **1993**, *2*, 113–118. [[CrossRef](#)]
37. Taylor, D.L.; Houston, S. A bioinformatics pipeline for sequence-based analyses of fungal biodiversity. In *Methods in Molecular Biology*; Xu, J.R., Bluhm, B.H., Eds.; Humana Press: Totowa, NJ, USA, 2011; Volume 722, pp. 141–155.
38. Timling, I.; Walker, D.A.; Nusbaum, C.; Lennon, N.J.; Taylor, D.L. Rich and cold: Diversity, distribution and drivers of fungal communities in patterned-ground ecosystems of the North American Arctic. *Mol. Ecol.* **2014**, *23*, 3258–3272. [[CrossRef](#)]
39. R Development Core Team. *R: A Language and Environment for Statistical Computing*; R Foundation for Statistical Computing: Vienna, Austria, 2017.
40. Zuur, A.F.; Ieno, E.N.; Walker, N.J.; Saveliev, A.A.; Smith, G.M. *Mixed Effects Models and Extensions in Ecology with R*; Springer: New York, NY, USA, 2009.
41. Flanagan, P.W.; Van Cleve, K. Nutrient cycling in relation to decomposition and organic matter quality in taiga ecosystems. *Can. J. For. Res.* **1983**, *13*, 795–817. [[CrossRef](#)]
42. Ruess, R.W.; Hendrick, R.L.; Bryant, J.P. Regulation of fine root dynamics by mammalian browsers in early successional Alaskan taiga forests. *Ecology* **1998**, *79*, 2706–2720, Erratum in **1999**, *80*, 1101. [[CrossRef](#)]
43. Gentili, F.; Wall, L.G.; Huss-Danell, K. Effects of phosphorus and nitrogen on nodulation are seen already at the stage of early cortical cell divisions in *Alnus incana*. *Ann. Bot.* **2006**, *98*, 309–315. [[CrossRef](#)]

44. Huss-Danell, K.; Gentili, F.; Valverde, C.; Wall, L.G.; Wiklund, A. Phosphorus is important in nodulation of actinorhizal plants and legumes. In *Nitrogen Fixation: Global Perspectives*; Finan, T., O'Brian, N., Layzell, D., Vessey, K., Newton, W., Eds.; CAB International: Wallingford, UK, 2002; pp. 163–166.
45. Mitchell, J.S.; Ruess, R.W. N₂-fixing alder (*Alnus viridis* spp. *fruticosa*) effects on soil properties across a secondary successional chronosequence in interior Alaska. *Biogeochemistry* **2009**, *95*, 215–229. [[CrossRef](#)]
46. Molina, R. Ectomycorrhizal specificity in the genus *Alnus*. *Can. J. Bot.* **1981**, *59*, 325–334. [[CrossRef](#)]
47. Kennedy, P.G.; Garibay-Orijel, R.; Higgins, L.M.; Angeles-Arguiz, R. Ectomycorrhizal fungi in Mexican *Alnus* forests support the host co-migration hypothesis and continental-scale patterns in phylogeography. *Mycorrhiza* **2011**, *21*, 559–568. [[CrossRef](#)] [[PubMed](#)]
48. Moreau, P.A.; Peintner, U.; Gardes, M. Phylogeny of the ectomycorrhizal mushroom genus *Alnicola* (Basidiomycota, Cortinariaceae) based on rDNA sequences with special emphasis on host specificity and morphological characters. *Mol. Phylogenet. Evolut.* **2006**, *38*, 794–807. [[CrossRef](#)] [[PubMed](#)]
49. Rochet, J.; Moreau, P.A.; Manzi, S.; Gardes, M. Comparative phylogenies and host specialization in the alder ectomycorrhizal fungi *Alnicola*, *Alpova* and *Lactarius* (Basidiomycota) in Europe. *BMC Evolut. Biol.* **2011**, *11*. [[CrossRef](#)] [[PubMed](#)]
50. Bogar, L.M.; Kennedy, P.G. New wrinkles in an old paradigm: Neighborhood effects can modify the structure and specificity of *Alnus*-associated ectomycorrhizal fungal communities. *FEMS Microbiol. Ecol.* **2013**, *83*, 767–777. [[CrossRef](#)] [[PubMed](#)]
51. Bolan, N.S. A critical review on the role of mycorrhizal fungi in the uptake of phosphorus by plants. *Plant Soil* **1992**, *134*, 189–207. [[CrossRef](#)]
52. Cairney, J.W.G. Intraspecific physiological variation: Implications for understanding functional diversity in ectomycorrhizal fungi. *Mycorrhiza* **1999**, *9*, 125–135. [[CrossRef](#)]
53. Cairney, J.W.G. Ectomycorrhizal fungi: The symbiotic route to the root for phosphorus in forest soils. *Plant Soil* **2011**, *344*, 51–71. [[CrossRef](#)]
54. Wurzburger, N.; Bellenger, J.P.; Kraepiel, A.M.L.; Hedin, L.O. Molybdenum and phosphorus interact to constrain asymbiotic nitrogen fixation in tropical forests. *PLoS ONE* **2012**, *7*. [[CrossRef](#)]
55. Agerer, R. Exploration types of ectomycorrhizae: A proposal to classify ectomycorrhizal mycelial systems according to their patterns of differentiation and putative ecological importance. *Mycorrhiza* **2001**, *11*, 107–114. [[CrossRef](#)]
56. Alvarez, M.; Huygens, D.; Díaz, L.M.; Villanueva, C.A.; Heyser, W.; Boeckx, P. The spatial distribution of acid phosphatase activity in ectomycorrhizal tissues depends on soil fertility and morphotype, and relates to host plant phosphorus uptake. *Plant Cell Environ.* **2012**, *35*, 126–135. [[CrossRef](#)]
57. Colpaert, J.V.; Van Tichelen, K.K.; Van Assche, J.A.; Van Laere, A. Short-term phosphorus uptake rates in mycorrhizal and non-mycorrhizal roots of intact *Pinus sylvestris* seedlings. *New Phytol.* **1999**, *143*, 589–597. [[CrossRef](#)]
58. Rineau, F.; Garbaye, J. Does forest liming impact the enzymatic profiles of ectomycorrhizal communities through specialized fungal symbionts? *Mycorrhiza* **2009**, *19*, 493–500. [[CrossRef](#)] [[PubMed](#)]
59. van Aarle, I.M.; Plassard, C. Spatial distribution of phosphatase activity associated with ectomycorrhizal plants is related to soil type. *Soil Biol. Biochem.* **2010**, *42*, 324–330. [[CrossRef](#)]
60. Turner, B.L.; Papházy, M.J.; Haygarth, P.M.; McKelvie, I.D. Inositol phosphates in the environment. *Philos. Trans. Royal Soc. B Biol. Sci.* **2002**, *357*, 449–469. [[CrossRef](#)]
61. Dalai, R.C. Soil Organic Phosphorus. In *Advances in Agronomy*; Brady, N.C., Ed.; Academic Press: New York, NY, USA, 1977; Volume 29, pp. 83–117.
62. Pertea, G.; Huang, X.; Liang, F.; Antonescu, V.; Sultana, R.; Karamycheva, S.; Lee, Y.; White, J.; Cheung, F.; Parvizi, B.; et al. TIGR gene indices clustering tools (TGICL): A software system for fast clustering of large EST datasets. *Bioinformatics* **2003**, *19*, 651–652. [[CrossRef](#)]
63. Huang, X.; Madan, A. CAP3: A DNA sequence assembly program. *Genome Res.* **1999**, *9*, 868–877. [[CrossRef](#)] [[PubMed](#)]
64. Altschul, S.F.; Madden, T.L.; Schäffer, A.A.; Zhang, J.; Zhang, Z.; Miller, W.; Lipman, D.J. Gapped BLAST and PSI-BLAST: A new generation of protein database search programs. *Nucleic Acids Res.* **1997**, *25*, 3389–3402. [[CrossRef](#)]
65. Edgar, R.C. MUSCLE: Multiple sequence alignment with high accuracy and high throughput. *Nucleic Acids Res.* **2004**, *32*, 1792–1797. [[CrossRef](#)]

66. Stamatakis, A.; Hoover, P.; Rougemont, J. A rapid bootstrap algorithm for the RAxML web servers. *Syst. Biol.* **2008**, *57*, 758–771. [[CrossRef](#)]
67. Taberlet, P.; Gielly, L.; Pautou, G.; Bouvet, J. Universal primers for amplification of three non-coding regions of chloroplast DNA. *Plant Mol. Biol.* **1991**, *17*, 1105–1109. [[CrossRef](#)]



© 2019 by the authors. Licensee MDPI, Basel, Switzerland. This article is an open access article distributed under the terms and conditions of the Creative Commons Attribution (CC BY) license (<http://creativecommons.org/licenses/by/4.0/>).